Application of Statistical Tools to Optimize a Dual Source Electrical High Dc Resistance Bridge

MAPAN-Journal of Metrology Society of India (September 2023) 38(3):573–581
https://doi.org/10.1007/s12647-023-00665-7

ORIGINAL PAPER

Application of Statistical Tools to Optimize a Dual Source Electrical High Dc Resistance Bridge

I. Mihai and F. Galliana*

Department of Applied Metrology and Engineering, National Institute of Metrological Research (INRIM), Strada Delle Cacce 91, 10135 Turin, Italy

Received: 30 March 2023 / Accepted: 15 May 2023 / Published online: 25 June 2023

Abstract: At the Istituto Nazionale di Ricerca Metrologica (INRIM), a commercial dual source high resistance bridge has been optimized by means of the application of statistical tools and of the analysis of measurements distributions. These tools help to achieve the best precision for resistance ratio measurements in the range 10 TΩ ÷ 100 TΩ. A measurement procedure consisting of multiple steps, in which at each one the value of the resistor under calibration is updated and has been considered the best one. With this procedure, at the third step, the lowest standard deviation of the mean and the measurements distribution approximately normal are obtained regardless of the settle time, of the resistance ratio, of the measurement voltages and of the resistors under comparison. This comes from the achievement of the white noise regime and from a bridge balance close to the ideal. This measurement procedure therefore allows also to achieve the lowest measurement uncertainty due to the minimization of the type A uncertainty. The Allan variance and the power spectral density were used to identify the white noise analyzing the detector readings. Strict triangulation rules were also established and applied to validate both the measurement process and the chosen model to extrapolate the values of the standard resistors at low voltages.

Keywords: High dc resistance measurements; Dual source Wheatstone bridge; Allan variance; Power spectral density; Gaussian distribution; Triangulation rule; White noise; Measurement uncertainty

1. Introduction

A common goal in metrology is the minimization of the systematic errors that affect the measurement precision. In electrical metrology, systematic errors can come from noises, mainly the *1/f* one, due to the electronics of the modern instrumentation. When such noises appear, the measurements are correlated and therefore the classical variance cannot be applied [1]. The Allan variance (AV) and the power spectral density (PSD), common in time and frequency metrology, were also used in low-frequency electrical metrology to characterize dc nanovoltmeters [2], to investigate the noise in Zener-based voltage standards [3] and to optimize a potentiometric system [4]. These tools allow identifying the white noise regime where the measurements are independent, and therefore, the classical mean and standard deviation of the mean can be applied. Triangulation rules were instead applied to check impedance comparison bridges [5] and to reproduce the dc electrical resistance unit at high level [6], respectively. In our work, strict triangulation rules were used to validate both the measurement process and the choice of a polynomial model to extrapolate the values of the standard resistors at low voltages by means of the INRIM CCC software [7]. All the measurements are available at: https://zenodo.org/record/7760237#.ZBwT8fbMKM9.

1.1. The DSB High Dc Resistance Bridge

Main National Measurement Institutes calibrate standard resistors from 10 MΩ to 100 TΩ and above by means of the dual source bridge (DSB) equipped with two dc voltage sources in the active arms of a Wheatstone bridge and a detector to seek the bridge balance [8–13]. The two e calibrators supply the voltages V_x and V_s, respectively, in the same ratio of the resistors R_x and R_s under comparison. The currents in R_x and R_s are in opposition and the bridge is balanced when their difference is null. As an ideal balance

*Corresponding author, E-mail: f.galliana@irim.it

cannot be achieved, the detector measures the residual unbalance current to calculate V_s. The R_x value is given by:

$$R_x = R_s\left(\frac{V_x}{V_s}\right) \quad (1)$$

The bridge balance can be sought also by means of voltage detection [12, 13]. Although this method is widely described in literature, noises at the detector and measurement waiting times according to the resistors typology are not yet exhaustively investigated. Our work has tried to fill these lacks by applying the AV, the PSD, the analysis of the measurements distributions and of strict triangulation rules. This activity has allowed identifying the white noise regime, where the measurements are not affected by the *1/f* noise in order to achieve the best performance of a commercial DSB.

1.2. The INRIM Commercial DSB High Dc Resistance Bridge

For high resistance measurements, at the Istituto Nazionale di Ricerca Metrologica (INRIM) operate two systems [10]. The first is based on a dc voltage calibrator and on a multimeter. It is used for calibration of resistors in the range 1 GΩ ÷ 1 TΩ. The second is a DSB, used for calibration in the range 100 GΩ ÷ 100 TΩ. Both systems were validated through their successfully participation at the comparisons [14, 15]. At INRIM is also available an automatic commercial DSB operating from 100 kΩ to 1 PΩ provided by the manufacturer with coaxial cables for the resistors connections. The bridge software was updated twice according to the INRIM advice [16, 17]. In [17], a description of the measurement modes available by the bridge (single measurement and multiple measurements with the auto update process) and the result of a compatibility test at 100 TΩ were given.

2. Measurements

Three ultra-high value resistors were involved in the measurements that followed the sequence of Fig. 1. The MI[1] resistors are based on a bulk resistive element while the Gdl[2] resistor is based on a resistance network.

In Table 1, the resistance ratio measurements according to Fig. 1 with the indication of the evaluated mean ratios and standard deviations of the mean [18] are reported.

The first ratio measurements were made by means of the single measurement mode at a settle time 3τ (time constant τ 600 s) at 250 V, 500 V, 750 V and 1000 V.

[1] Measurement International (MI).

[2] Guildline (Gdl).

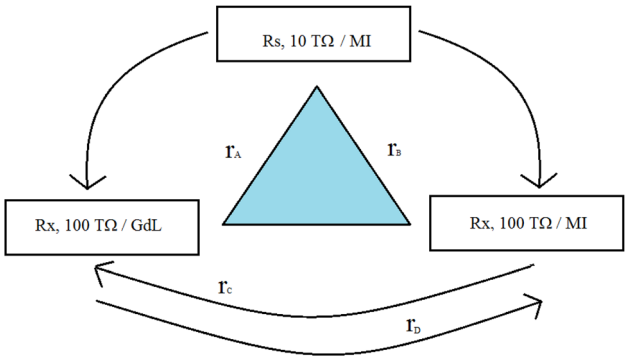

Fig. 1 Resistance ratio comparisons made with the commercial DSB

Successively, the same measurements were made by means of the multiple measurements mode with the auto update process in four steps at increasing settle times (from ½ τ to 3τ). This choice was made to expedite the measurements that anyhow lasted for several days. In the auto update process, the R_x value is changed at each step approaching its best estimate as at each step the current at the detector approaches zero. In the first two steps, the detector was treated as a picoammeter taking into account its calibration value, while at the third step, it was treated as a null detector. As the standard resistors involved in the comparisons were not calibrated at low voltages, their values at these voltages were extrapolated by means of prediction intervals using the INRIM CCC software [7]. All the measurements were made in the white noise regime having established the number of the detector readings to achieve this regime (see par. 3.2). Table 2 reports the results of the comparison A, Fig. 1.

Figures 2a, 2b and 2c show the values of the standard deviation of the mean vs. the measurement settle times for the comparisons B, C and D with the multiple measurements mode with the auto update process for each measurement voltage.

3. Errors Analysis

The statement in [19] that limits the DSB to 1 PΩ and the failure of a compatibility test at the same value between the two INRIM DSB bridges (the INRIM developed and the commercial one [20]) demanded an analysis of the systematic errors affecting this technique at ultra-high resistance values.

3.1. Analysis of the Measurements Distributions

In Table 2 and in Figs. 2, the lowest standard deviations of the mean are observed at the third step. This is likely due to both a satisfactory bridge balance (close to zero current at

Table 1 Resistance ratio measurements according to Fig. 1

Comparisons		Ratio	Mean ratio $\overline{r}$	Standard deviation of the mean of the ratio s_r
A	R_s 10 TΩ MI R_x 100 TΩ Gdl	1:10	$\overline{r_A}$	s_{rA}
B	R_s 10 TΩ MI vs R_x 100 TΩ MI	1:10	$\overline{r_B}$	s_{rB}
C	R_s 100 TΩ MI vsR_x 100 TΩ Gdl		$\overline{r_C r_C}$	s_{rC}
D	R_s 100 TΩ Gdl R_x 100 TΩ MI		$\overline{r_D}$	s_{rD}

Table 2 Measurement results of the comparison A

Comparison A			Settle time (s)	Unbal. ($\times 10^{-6}$)	Voltage (V)	Ratio r ($\times 10^{-6}$)	s_{rA}($\times 10^{-6}$)
n	Task						
1	$r_{A0\ 250\ V}$	3τ	1800	40.001	250	20.161	693
2	$r_{A0\ 500\ V}$	3τ	1800	20.001	500	17.351	406
3	$r_{A0\ 750\ V}$	3τ	1800	13.334	750	17.987	344
4	$r_{A0\ 1000\ V}$	3τ	1800	10.001	1000	17.551	255
5	$r_{A1\ 250\ V}$	$^{1/2}$τ	300	40.001	250	18.121	1338
6	$r_{A2\ 250\ V}$	τ	600	–	250	20.554	1807
7	$r_{A3\ 250\ V}$	2τ	1200	–	250	18.143	**338**
8	$r_{A4\ 250\ V}$	3τ	1800	–	250	19.161	1167
9	$r_{A1\ 500\ V}$	$^{1/2}$τ	300	20.001	500	17.014	604
10	$r_{A2\ 500\ V}$	τ	600	–	500	18.183	629
11	$r_{A3\ 500\ V}$	2τ	1200	–	500	17.542	**156**
12	$r_{A4\ 500\ V}$	3τ	1800	–	500	14.520	335
13	$r_{A1\ 750\ V}$	$^{1/2}$τ	300	13.334	750	17.299	349
14	$r_{A2\ 750\ V}$	τ	600	–	750	16.859	298
15	$r_{A3\ 750\ V}$	2τ	1200	–	750	17.524	**91**
16	$r_{A4\ 750\ V}$	3τ	1800	–	750	16.842	496
17	$r_{A1\ 1000\ V}$	$^{1/2}$τ	300	10.001	1000	17.146	311
18	$r_{A2\ 1000\ V}$	τ	600	–	1000	18.718	197
19	$r_{A3\ 1000\ V}$	2τ	1200	–	1000	17.367	**81**
20	$r_{A4\ 1000\ V}$	3τ	1800	–	1000	16.320	251
21	$r_{A0\ 1000\ V}$	3τ	840	10.001	1000	17.384	193
22	$r_{A0\ 1000\ V}$	3τ	840	–	1000	17.359	186
23	$r_{A1\ 1000\ V}$	$^{1/2}$τ	140	–	1000	17.098	188
24	$_{rA2\ 1000\ V}$	τ	280	–	1000	17.455	248
25	$r_{A3\ 1000\ V}$	2τ	560	–	1000	18.287	**147**
26	$r_{A4\ 1000\ V}$	3τ	840	–	1000	17.484	358

The unbalance value is the initial closeness to the perfect bridge balance set programming a measurement sequence. Updating the value of the resistor under calibration the unbalance is automatically lowered at each step approaching at best the ideal bridge balance (i.e., zero current)

Bold values indicates the tasks in which the corresponding triangulation rule is satisfied

the detector) and to the white noise regime. These lowest standard deviations of the mean are observed regardless of the resistance ratio, of the resistors under comparison, of the measurement voltages and of the measurement settle time. To confirm the last statement, the tasks 23–26 of the comparison A (Table 2) were made also at τ 280 s and the lowest standard deviation of the mean is again observed at the third step. Figures 3a) to 3i) show the histograms of the comparisons A, B and D with the multiple measurements mode at 500 V. These histograms were made according to the Sturges rule [21].

$$b = 1 + 3.322 \times \log(N) \quad (2)$$

where b is the number of bins (intervals) and N is the measurements number. A better analysis is currently underway by means of the Kolmogorov–Smirnov test [22].

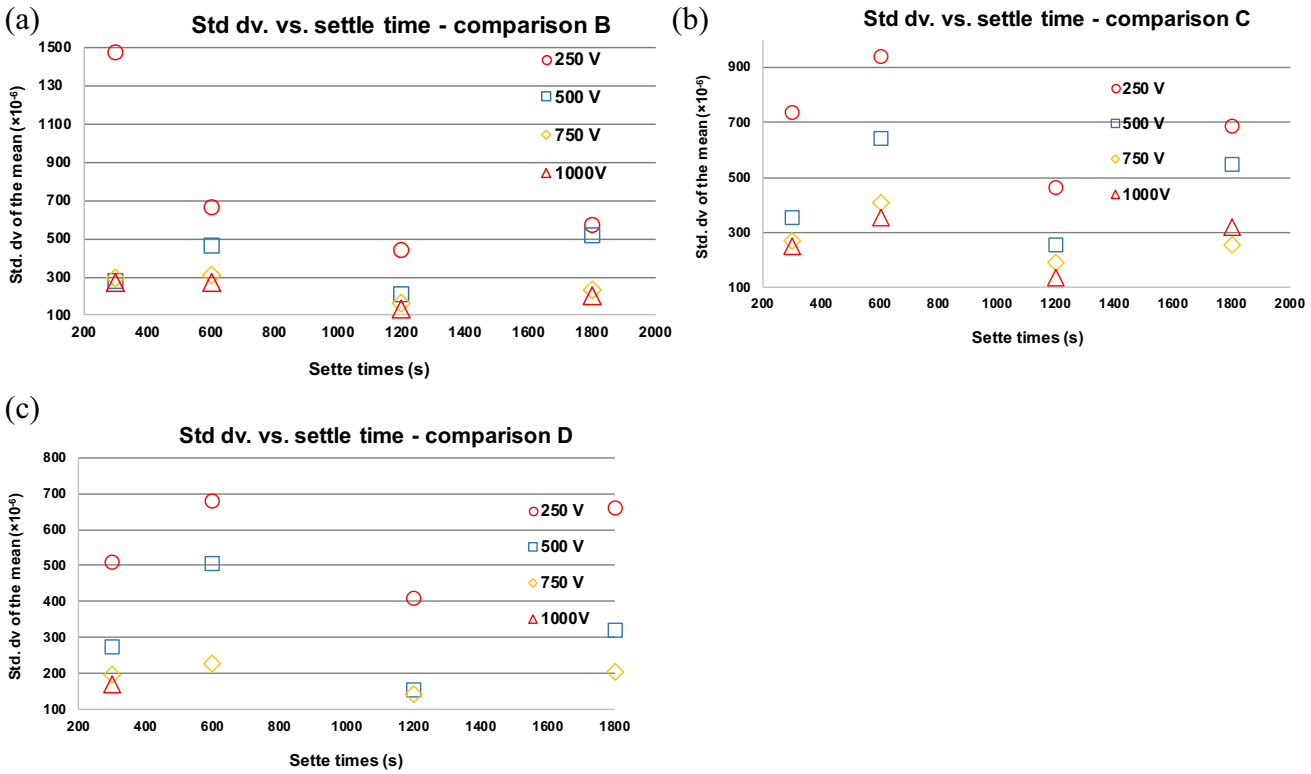

Fig. 2 **a** Standard deviation of the mean vs. measurement settle time for the comparison B. **b**. Standard deviation of the mean vs. measurement settle time for the comparison C. **c**. Standard deviation of the mean vs. measurement settle time for the comparison D in Fig. 1. The measurements at 1000 V were performed only at 300 s as for longer times the voltage on R_s was higher than 1050 V stopping the program

At the third step, the distributions are close to the Gaussian one.[3] The distributions corresponding to the first two steps and to the fourth one deviate from the Gaussian one, meaning that the measurements are affected by systematic errors. These are due in the first two steps, to the balance of the bridge far from the ideal while in the fourth step are due to the drift of the calibrators.

3.2. Application of the Allan Variance and of the Power Spectral Density

To apply the AV and the PSD to investigate the noises at the detector, its input current was converted to ± 2 V at its output and acquired by a digital fast Fourier transform (FFT) digital analyzer. Figure 4a, b, c, d, e, f, g and h shows the ADs and the PSDs of the comparisons *C* and *D* at 500 V. These graphs were obtained elaborating the detector readings by means of the Stable32 software [23].

In Figs. 4, the PSDs behavior inversely proportional to frequency reveals a *1/f* noise regime [1] in the range around 0.01 Hz ÷ 1 Hz. This noise is likely due to the dc voltage calibrators. At about 1 Hz, the *1/f* noise merges with the white noise, which lies around.

1 Hz ÷ 20 Hz. The AD and the standard deviation reach their minimum at integrating times around 0.64 s ÷ 1.28 s for measurements at voltages from 250 to 1000 V. No increase in accuracy can be gained at longer integrating times due to the *1/f* noise. By means of these estimators, it is then possible to establish the appropriate number of the detector readings to assure that the measurements are made in white noise regime. In this regime, the AD and the standard are linked by the:

$$= \sigma_x(N) = \frac{1}{\sqrt{N}|H_D(f)|}\sigma_y(\tau) \tag{3}$$

where N and $H_D(f)$ are, respectively, the number of the readings of the detector and its transfer function. In Table 3, the conversion from the AD minimum to the standard deviation of the signal at the detector and the appropriate number of its readings to operate in white noise regime are reported.

Par25 More precisely, they are close to the Student's distribution that, in turn, is close to the Gaussian one for a low number of measurements.

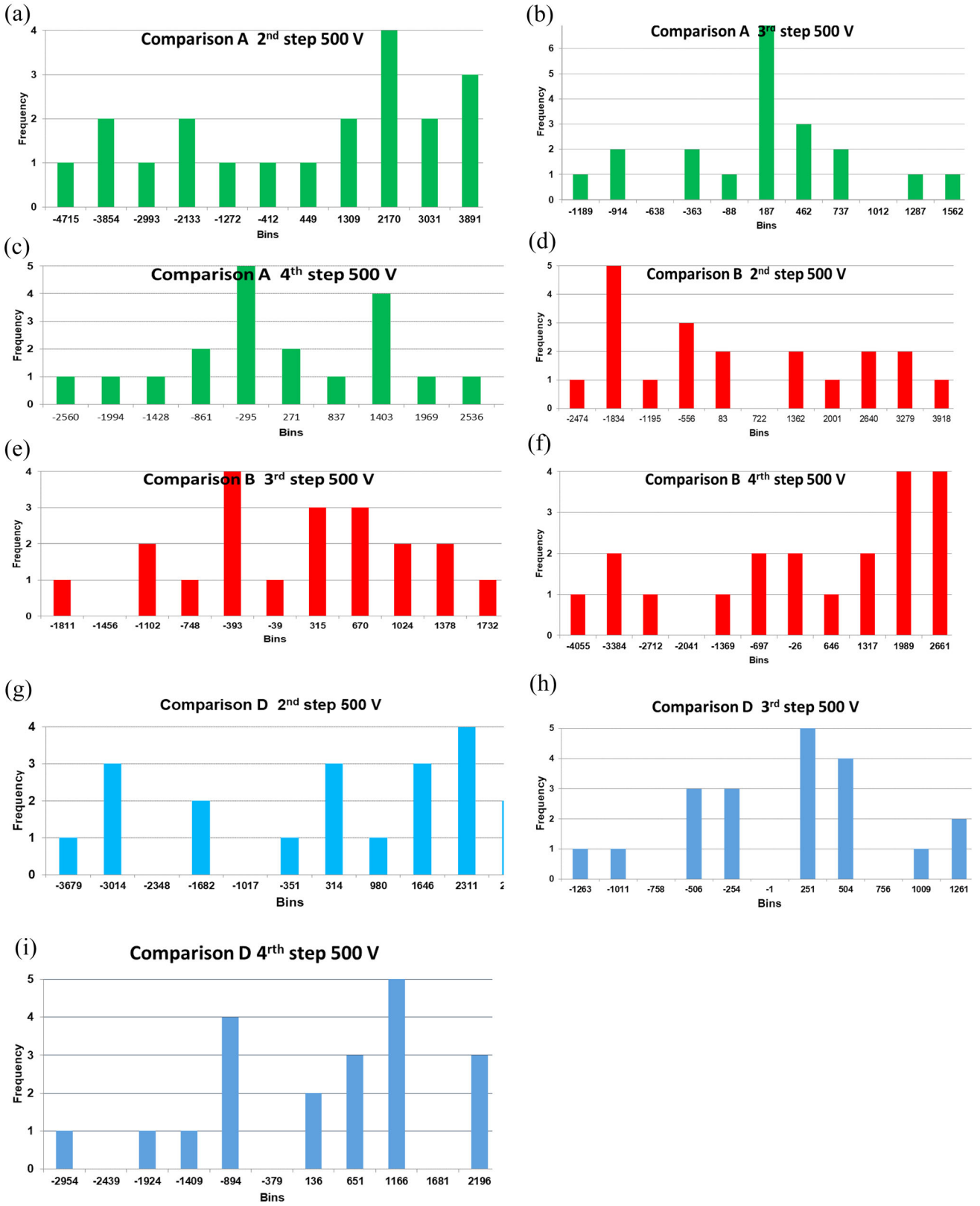

Fig. 3 **a** Comparison A, 2nd step, **b** Comparison A, 3rd step, **c**. Comparison A, 4th step, **d** Comparison B, 2nd step, **e** Comparison B, 3rd step, **f** Comparison B, 4th step, **g**. Comparison D, 2nd step, **h** Comparison D, 3rd step, **i** Comparison D, 4th step

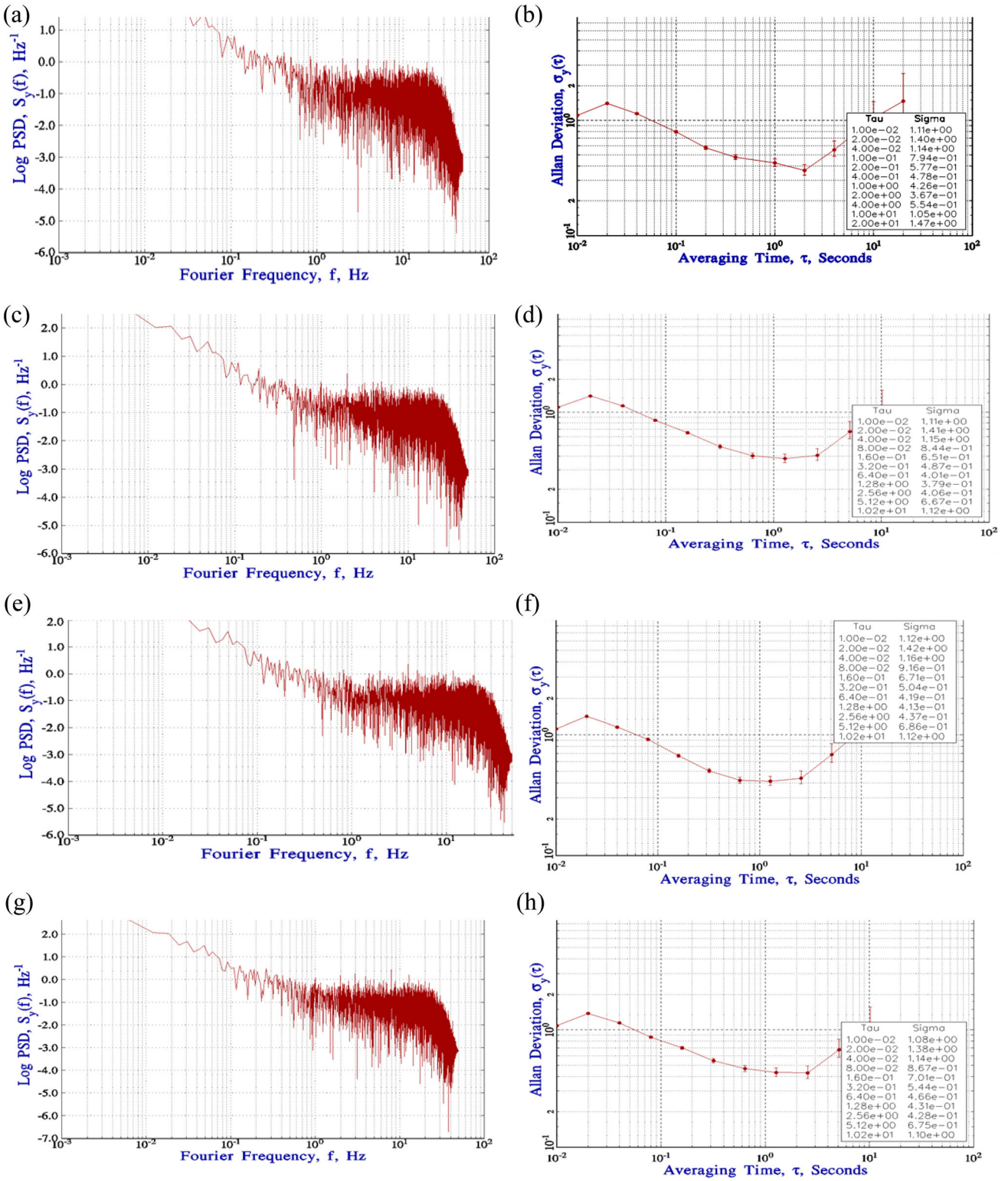

Fig. 4 **a** PSD, comparison C at + 500 V., **b** AD, comparison C at + 500 V., **c** PSD, comparison C at − 500 V., **d** AD, comparison C at − 500 V., **e** PSD, comparison D at + 500 V., **f** AD for the comparison D at + 500 V., **g** PSD for the comparison D at − 500 V., **h** AD for the comparison D at − 500 V

Table 3 Conversion from the minimum value of AD to the standard deviation of the signal at the detector and to the number of the detector readings in white noise regime

V	σ_y (τ) (mV)	$\sigma_x(N)$ (fA)	Detector readings (NPLC 20 ms)
250	0.43	0.5	64
500	0.39	0.7	32
750	0.41	0.7	32
1000	0.40	0.7	32

As the detector is set 1 PLC, the appropriate number of the detector readings to be in the white noise regime is evaluated by dividing by 20 ms the τ value corresponding to the lowest AD [17]

3.3. Application of Triangulation Rules

The fulfillment of strict triangulation rules, taking into account the lowest standard deviation of the mean (corresponding to the third step of the auto update process), allows to validate the measurement procedure and the chosen model to extrapolate the values of the standard resistors at low voltages. According to Fig. 1, it should be:

$$\overline{r_A} \cong \overline{r_B} \times \overline{r_C} \text{ or } \quad 1 - \frac{r_A}{r_B \times r_C} \times 10^6 \cong 0 \tag{4}$$

$$\text{and } \overline{r_B} \cong \overline{r_A} \times \overline{r_D} \text{ or } \quad 1 - \frac{r_A \times r_D}{r_B} \times 10^6 \cong 0 \tag{5}$$

The fulfillment of the following equations at the third step of the multiple mode, where the s_r are the lowest, was verified:

$$\text{(a)} \quad 1 - \frac{r_A}{r_B \times r_C} \times 10^6 < \sqrt{s_{rA}^2 + s_{rB}^2 + s_{rC}^2} \quad \text{(b)} \tag{6}$$

$$\text{and} \qquad \text{(a)} \quad 1 - \frac{r_A \times r_D}{r_B} \times 10^6 < \sqrt{s_{rA}^2 + s_{rB}^2 + s_{rD}^2} \quad \text{(b)} \tag{7}$$

This test allowed to check the correctness of the chosen measurement process in the most critical condition. The obtained results from our measurements are shown in Tables 4 and 5 where the measurements at the third step correspond to the tasks 7, 11, 15 and 19.

4. Discussion

To fully validate the measurement procedure, based on the auto update process, the triangulation rules corresponding to ratio measurements at the third step following the scheme in Fig. 1 have to be satisfied. If this condition holds (to be confirmed by other methods as Monte Carlo simulation), the vice versa has also to hold. According to this validation condition, our measurement process has not been yet fully validated. In fact, the triangulation rule of Eq. (6) at the third step was satisfied only at 250 V (task 7, in green, Table 4). The rule (7) at the same step was instead satisfied at 250 V, 500 V and 750 V (tasks 7, 11, 15, in green, Table 5). At 1000 V, the rule 7 was not tested as the comparison D was not made (see Table 2d). The RSS values (Eqs. (6)b and (7)b) at the step 3 are on the same order, while the corresponding values 6a and 7a differ at higher voltages than 250 V. The 6a values increase as the measurement voltage increases, while the same effect is not observed for the 7a values. Being $\overline{r_A}$ and $\overline{r_B}$ in both equations, $\overline{r_C}$ and $\overline{r_D}$ are not compatible presumably for an interchangeability error due to the different function (R_s or R_x) of the two 100 TΩ resistors in the comparisons C and D. For these two ratio measurements, the waiting times of the measurement have to be different as the bulk-based resistor, when acts as R_s, needs a longer time to allow a reliable measurement. On the other hand, at longer waiting times, drift and malfunctions of the dc calibrators, due to their overheating, can occur. These results should be extended in further measurements also up to 1 PΩ.

5. Conclusions

The measurement mode allowing the best performance of the commercial DSB in ultra-high dc resistance consists of multiple steps by means of the multiple measurements mode with the auto update process. The value at the third step is trustworthy as not depending on the settle/waiting time, on the ratio value, on the measurement voltages and on the resistors under comparison. The shape of the measurements distribution at this step, close to the Gaussian one, confirms this statement. The reliability of the value at the third step is due to the achievement of both a satisfactory close to zero current at the detector and of a white noise regime. At the same step, the lowest uncertainty of the resistance ratio measurements is also obtained. This result does not imply consequently that the value of the resistor under calibration at the third step is its best estimate, as other systematic errors, not depending by the bridge, may occur. Such errors come from the calibration value, from the drift and from the temperature effect of the standard resistor. The not completely satisfactory triangulation exercise suggests further investigations on the

Table 4 Triangulation results according to Eq. (6)

Task	Settle time (s)		Unbal. ($\times 10^{-6}$)	Voltage (V)	Equation 6 (a) ($\times 10^{-6}$) (b) RSS ($\times 10^{-6}$)	
Single measurement mode						
1	3τ	1800	40.001	250	− 3015	1286
2	3τ	1800	20.001	500	− 422	590
3	3τ	1800	13.334	750	− 5549	472
4	3τ	1800	10.001	1000	− 7536	336
Multiple measurements mode						
5	$^{1/2}\tau$	300	40.001	250	− 336	2123
6	τ	600	–	–	− 223	2142
7	2τ	1200	–	–	**− 549**	**723**
8	3τ	1800	–	–	− 6071	1471
9	$^{1/2}\tau$	300	20.001	500	− 2863	753
10	τ	600	–	–	− 3952	1012
11	2τ	1200	–	–	− 2053	366
12	3τ	1800	–	–	2908	825
13	$^{1/2}\tau$	300	13.334	750	− 5610	532
14	τ	600	–	–	− 2797	594
15	2τ	1200	–	–	− 4139	265
16	3τ	1800	–	–	− 2079	604
17	$^{1/2}\tau$	300	10.001	1000	− 6798	484
18	τ	600	–	–	− 7446	489
19	2τ	1200	–	–	− 6006	208
20	3τ	1800	–	–	− 4890	454

RSS: Ratio Sum Square

Bold values indicates the tasks in which the corresponding triangulation rule is satisfied

Table 5 Triangulation results according to the Eq. (7)

Task	Settle time (s)		Unbal. ($\times 10^{-6}$)	Voltage (V)	Equation 7a) ($\times 10^{-6}$) 7b) RSS ($\times 10^{-6}$)	
Single measurement mode						
1	3τ	1800	40,001	250	− 2927	1368
2	3τ	1800	20,001	500	1615	582
3	3τ	1800	13,334	750	528	465
4	3τ	1800	10,001	1000	− 625	319
Multiple measurements mode						
5	$^{1/2}\tau$	300	40,001	250	− 878	2056
6	τ	600	–	–	− 240	2042
7	2τ	1200	–	–	**− 579**	**689**
8	3τ	1800	–	–	− 6865	1458
9	$^{1/2}\tau$	300	20,001	500	783	720
10	τ	600	–	–	− 2480	933
11	2τ	1200	–	–	**− 23**	**303**
12	3τ	1800	–	–	2921	695
13	$^{1/2}\tau$	300	13,334	750	244	501
14	τ	600	–	–	501	489
15	2τ	1200	–	–	**168**	**235**
16	3τ	1800	–	–	925	585
17	$^{1/2}\tau$	300	10,001	1000	682	448

Bold values indicates the tasks in which the corresponding triangulation rule is satisfied

correct waiting times according to the typology and function of the resistors under comparison and on the minimization of the drift of the calibrators at long waiting times. Further weakness of the commercial bridge could be its guarding system based on coaxial connections. As the result of the comparison at 100 TΩ [22] partially conflicts with the results of this paper, after an analysis of the errors also of the INRIM DSB bridge, a new comparison at the same value has to be repeated to confirm the current results. Further outcomes will be the applying of the triangulation rules till to 1 PΩ and the equipment of the bridge with a triaxial guarding system to verify if this change can further improve the bridge performance. The statistical tools applied in this paper can be applied when the compatibility in inter-laboratories comparisons fails and in other low-frequency electrical quantities.

Funding Open access funding provided by Istituto Nazionale di Ricerca Metrologica within the CRUI-CARE Agreement.

References

[1] D.W. Allan, Should the classical variance be used as a basic measure in standards metrology? IEEE Trans. Instrum. Meas., **36** (1987) 646-654.
[2] T.J. Witt, Using the Allan variance and power spectral density to characterize DC nanovoltmeters. IEEE Trans. Instrum. Meas., **50**(2) (2001) 445-448.
[3] T.J. Witt and D. Reymann, Using power spectra and Allan variance to characterise the noise of Zener–diode voltage standards. IEEE Proc-Sci Meas. Technol., **147**(4) (2000) 177-182.
[4] I. Mihai and G. Marullo, Reedtz Optimization of a potentiometric measurement system by calculation of the Allan variance, Proceedings Conf. Conf. Prec. Elec. Meas. CPEM Ottawa, Canada (2002) pp. 48-49.
[5] K. Musiol and M. Kampik, Metrological triangles in impedance comparisons. Measurement, **148**(106908) (2019) 1-7.
[6] I. Mihai, Reproduction of the Unit of Electrical Resistance at the Highest Level of Accuracy, PhD Thesis, Politecnico of Turin and University Polytechnica of Bucharest, (2004).
[7] A. Malengo and F. Pennecchi, A weighted total least–squares algorithm for any fitting model with correlated variables. Metrogia, **50** (2013) 654-662.
[8] L.C.A. Henderson, A new technique for the automatic measurement of high value resistors. J. Phys. E. Sci. Instrum., **20** (1987) 492-495.
[9] D.G. Jarrett, Automated guarded bridge for calibration of multimegohm standard resistors from 1 MΩ to 1 TΩ IEEE Trans. Instr. Meas., **46**(2) (1997) 325–328.
[10] F. Galliana, P.P. Capra and E. Gasparotto, Evaluation of two different methods to calibrate ultra–high value resistors at INRIM. IEEE Trans. Meas., **59**(11) (2010) 1-6.
[11] I. Leniček, D. Ilić and L. Ferković, High value resistance comparison using modified Wheatstone bridge based on current detection. Measurement, **46**(10) (2013) 4388-4393.
[12] G. Rietveld and J.H.N. van der Beek, Automated high-ohmic resistance bridge with voltage and current null–detection. IEEE Trans. Instrum. Meas., **62**(6) (2013) 1760-1765.
[13] Ö. Erkan et al, Active Guarded Wheatstone Bridge for High Resistance Measurements Up to 100 TΩ at TÜBİTAK UME, Proceedings Conf. Prec. Elec. Meas. CPEM, Paris, France (2018) pp. 1-2, https://doi.org/10.1109/CPEM.2018.8501194.
[14] R.F. Dziuba and D.G. Jarrett, Final report on key comparison CCEM–K2 of resistance standards at 10 MΩ and 1 GΩ, 002. Metrologia, **39** (2001) 01001. https://doi.org/10.1088/0026-1394/39/1A/1.
[15] B. Jeckelmann, J.H. van der Beek, P.P. Capra, P. Chrobok, L. Cirneanu, E. Dudek, Ö. Erkan, I. Flouda, F. Galliana, I. Godinho and O. Gunnarsson, Final report on supplementary comparison EURAMET.EM–S32: Comparison of resistance standards at 1 TΩ and 100 TΩ, Metrogia **50** (2013). https://doi.org/10.1088/0026-1394/50/1A/01008
[16] F. Galliana, P.P. Capra and E. Gasparotto. Evaluation of the measurement capabilities of a high performance commercial high resistance bridge by means of the comparison with two validated high resistance measurement methods, Proc. 17th Int. Congr. Metrology, France (2015) pp. 1-4. https://doi.org/10.1051/metrology/20150010001.
[17] I. Mihai, P. Capra and F. Galliana, Evaluation of a commercial high resistance bridge and methods to improve its precision Metrol. Meas. Syst., **29**(4) (2022) 701-718.
[18] JCGM 100:2008 Evaluation of measurement data – Guide to the expression of uncertainty in measurement First edition.
[19] Y. Kwang Min, D.G. Jarrett, A.F. Rigosi, S.U. Payagala and M.E. Kraft, Comparison of multiple methods for obtaining PΩ resistances with low uncertainties. IEEE Trans. Instrum. Meas., **69**(6) (2020) 3729-3737.
[20] F. Galliana, P.P. Capraa and I. Mihai, Measurement comparison between a commercial high resistance bridge and validated systems at ultra–high resistance values. Proc. 20th TC–4 Workshop on ADC and DAC Modelling and Testing, Palermo, Italy, (2020) pp. 379-384.
[21] H.A. Sturges, The choice of a class interval. Journal of the American Statistical Association, **21**(153) (1926) 65-66. https://doi.org/10.1080/01621459.1926.10502161.JSTOR2965501.
[22] Lopes, R.H.C. Kolmogorov–Smirnov Test. In: M. Lovric, (eds) International Encyclopedia of Statistical Science. Springer, Berlin, Heidelberg, (2011).
[23] Hamilton Technical Services Stable32 User Manual, (2008). http://www.stable32.com.